BMTP-11 is active in preclinical models of human osteosarcoma and a candidate targeted drug for clinical translation

Valerae O. Lewis[a,1,2], Eswaran Devarajan[a,1], Marina Cardó-Vila[b,c], Dafydd G. Thomas[d,e], Eugenie S. Kleinerman[f], Serena Marchiò[b,c,g,h], Richard L. Sidman[i,2], Renata Pasqualini[b,c,2,3], and Wadih Arap[b,j,2,3]

[a]Department of Orthopedic Oncology, Division of Surgery, The University of Texas M.D. Anderson Cancer Center, Houston, TX 77030; [b]University of New Mexico Comprehensive Cancer Center, Albuquerque, NM 87106; [c]Division of Molecular Medicine, Department of Internal Medicine, University of New Mexico School of Medicine, Albuquerque, NM 87131; [d]University of Michigan Comprehensive Cancer Center, Ann Arbor, MI 48109; [e]Department of Pathology, University of Michigan, Ann Arbor, MI 48109; [f]Department of Pediatrics, The University of Texas M.D. Anderson Cancer Center, Houston, TX 77030; [g]Department of Oncology, University of Torino, 10060 Candiolo, Torino, Italy; [h]Candiolo Cancer Institute, IRCCS, 10060 Candiolo, Torino, Italy; [i]Department of Neurology, Harvard Medical School, Boston, MA 02115; and [j]Division of Hematology/Oncology, Department of Internal Medicine, University of New Mexico School of Medicine, Albuquerque, NM 87131

Contributed by Richard L. Sidman, June 12, 2017 (sent for review March 28, 2017; reviewed by Dempsey S. Springfield and Kristy L. Weber)

Osteosarcoma occurs predominantly in children and young adults. High-grade tumors require multidisciplinary treatment consisting of chemotherapy in the neoadjuvant and adjuvant settings, along with surgical intervention. Despite this approach, death from respiratory failure secondary to the development and progression of pulmonary metastases remains a significant problem. Here, we identify the IL-11 receptor α subunit (IL-11Rα) as a cell surface marker of tumor progression that correlates with poor prognosis in patients with osteosarcoma. We also show that both IL-11Rα and its ligand, IL-11, are specifically up-regulated in human metastatic osteosarcoma cell lines; engagement of this autocrine loop leads to tumor cell proliferation, invasion, and anchorage-independent growth in vitro. Consistently, IL-11Rα promotes lung colonization by human metastatic osteosarcoma cells in vivo in an orthotopic mouse model. Finally, we evaluate the IL-11Rα–targeted proapoptotic agent bone metastasis-targeting peptidomimetic (BMTP-11) in preclinical models of primary intratibial osteosarcomas, observing marked inhibition of both tumor growth and lung metastases. This effect was enhanced when BMTP-11 was combined with the chemotherapeutic drug gemcitabine. Our combined data support the development of approaches targeting IL-11Rα, and establish BMTP-11 as a leading drug candidate for clinical translation in patients with high-risk osteosarcoma.

BMTP-11 | IL-11Rα | osteosarcoma | mouse models | target therapy

Osteosarcoma is a tumor of bone with peak incidence occurring at age 10–20 y (1). Over the past quarter century, the 5-y survival rate has remained stagnant at ∼60–65% for patients with primary osteosarcoma and ∼20–25% for patients with metastatic disease (2), with few therapeutic options available. The current standard of care for high-grade osteosarcoma is an aggressive combination of high-dose methotrexate with doxorubicin (Adriamycin) and cisplatin (MAP) in the neoadjuvant and adjuvant settings, complemented by surgery when possible (2). Systemic treatment options have remained unchanged for the last 30 y. With the exception of mifamurtide (3, 4), which has been approved for use in the European Union and Israel—but, unfortunately, not the United States—the pipeline of cytotoxic drugs against osteosarcoma has essentially been dry. Recently, the EURAMOS-1 clinical trial demonstrated that the addition of ifosfamide plus etoposide to standard MAP (MAPIE) did not affect overall survival in patients with poor response (defined as ≤90% tumor necrosis to induction therapy), whereas PEGylated IFN alfa-2b maintenance provided only a modest (nonsignificant) improvement in the event-free survival of patients with good response (5).

The widespread use of gemcitabine in sarcoma management, along with encouraging initial reports of gemcitabine plus docetaxel (GEMDOX) in pediatric osteosarcoma, prompted a formal evaluation in clinical trials. Despite some controversy, this regimen has been recently reported as somehow active against relapsed and unresectable high-grade tumors (6). Promisingly, the addition of bevacizumab, an anti-vascular endothelial growth factor A antibody, to paclitaxel and gemcitabine (TAG) seems to improve the efficacy of GEMDOX in very high-risk osteosarcomas (7). Moreover, a few biological agents are also being evaluated in clinical trials, including monoclonal antibodies against insulin-like growth factor receptor 1, angiogenesis inhibitors such as sorafenib and pazopanib, small-molecule inhibitors of the mammalian target of rapamycin such as temsirolimus and everolimus, and immune checkpoint inhibitors (8–10).

Significance

In its metastatic/recurrent presentation, osteosarcoma is a high-risk tumor with poor management, essentially unchanged over the past 25 years. Osteosarcoma is a relatively rare cancer; however, because it affects predominantly teenagers and young adults, it is a leading disease-related cause of death and a major contributor to years of life lost in this age group. Here, we demonstrate the prognostic value of IL-11Rα in osteosarcoma progression and patient survival. We also report preclinical studies with the IL-11Rα–targeted peptidomimetic bone metastasis-targeting peptidomimetic (BMTP-11) as a therapeutic agent, either alone or in combination with gemcitabine, in both primary tumor and metastatic disease models. This study demonstrates successful applications directed against the IL-11Rα:IL-11 molecular axis in preclinical models of osteosarcoma.

Author contributions: V.O.L., E.D., M.C.-V., D.G.T., S.M., R.L.S., R.P., and W.A. designed research; V.O.L., E.D., and D.G.T. performed research; E.S.K. and R.L.S. contributed new reagents/analytic tools; V.O.L., E.D., M.C.-V., D.G.T., S.M., R.L.S., R.P., and W.A. analyzed data; and V.O.L., E.D., M.C.-V., S.M., R.L.S., R.P., and W.A. wrote the paper.

Reviewers: D.S.S., Massachusetts General Hospital; and K.L.W., University of Pennsylvania Perelman School of Medicine.

Conflict of interest statement: R.P. and W.A. are founders and equity stockholders of Alvos Therapeutics (Arrowhead Pharmaceuticals Research Corporation). Arrowhead Pharmaceuticals has licensed rights to patents and technologies described in this article. R.P. and W.A. are inventors on patent applications and intellectual property related to this work and will be entitled to standard royalties if licensing and/or commercialization occurs. The University of New Mexico Health Sciences Center manages and monitors these arrangements, along with the University of Texas M.D. Anderson Cancer Center.

Freely available online through the PNAS open access option.

[1]V.O.L. and E.D. contributed equally to this work.

[2]To whom correspondence may be addressed. Email: volewis@mdanderson.org, richard_sidman@hms.harvard.edu, rpasqual@salud.unm.edu, or warap@salud.unm.edu.

[3]R.P. and W.A. contributed equally to this work.

This article contains supporting information online at www.pnas.org/lookup/suppl/doi:10.1073/pnas.1704173114/-/DCSupplemental.

In previous work, our research group (11) and other investigators (12–14) have independently demonstrated that the IL-11:IL-11Rα axis regulates a downstream program through the signal transduction and activator of transcription 3 (STAT3) in bone tumors, such as primary osteosarcoma and nonosteosarcoma bone metastasis. Within this context, here we evaluate the activity of an IL-11Rα–targeted agent, bone metastasis-targeting peptidomimetic (BMTP)-11, as a potential drug candidate against osteosarcoma. We demonstrate that IL-11Rα is overexpressed in osteosarcoma tumor cells and is functionally relevant in osteosarcoma progression, and that BMTP-11 delays the growth of both primary tumors and lung metastases in preclinical orthotopic models of human osteosarcoma, with improved efficacy when combined with gemcitabine. Taken together, our experimental findings establish the IL-11:IL-11Rα pathway as a functionally active axis for therapeutic intervention in human osteosarcoma, and provide preclinical proof of concept for evaluation of BMTP-11 in first-in-human clinical trials.

Results and Discussion

IL-11Rα Expression Increases During Metastatic Progression and Correlates with Poor Prognosis in Patients with Osteosarcoma. The patterns and levels of IL-11Rα expression in human osteosarcoma were evaluated by immunohistochemistry (IHC) on a tissue microarray (TMA) prepared with surgical specimens of primary tumors ($n = 18$) and lung metastases ($n = 27$). Staining was analyzed as both signal intensity (on a scale of 0–4) and distribution (proportion of IL-11Rα–positive cells ranked on a scale of 0–4). Lung metastases showed a significantly higher IL-11Rα mean intensity score (2.8 vs. 1.8, $P < 0.01$; Fig. 1*A*) compared with the primary tumors, as well as a trend toward more IL-11Rα–positive cells (2.9 vs. 2.5, $P = 0.06$; Fig. 1*B*). Thus, in osteosarcoma patients, metastases express higher levels of IL-11Rα than primary tumors. This finding extends previous investigations supporting the validity of IL-11Rα as a biomarker in high-risk osteosarcomas (11, 13) and in bone metastases from other tumors (12, 15).

In the present study, survival data were available for subsets of patients with primary osteosarcoma ($n = 14$) and lung metastasis ($n = 15$). For correlation studies, patients with primary osteosarcoma were sorted into two groups with a low (<2) or high (≥2) IL-11Rα intensity score. Lower 10-y survival (17% vs. 63%) was observed in the high-intensity group (Fig. 1*C*); the difference between groups was calculated by Cox's F test ($P = 0.056$) and the log-rank test ($P = 0.15$). Correlation studies performed on IL-11Rα distribution (≤2 vs. ≥3) confirmed a similar trend, with a 10-y overall survival of 29% in the high-distribution group, compared with 52% in the low-distribution group (Fig. 1*D*). These results show that patients with higher levels of IL-11Rα in their primary tumor cells have a worse prognosis compared with patients with lower levels of IL-11Rα.

For lung metastasis, there were no discernable differences in overall patient survival based on either the distribution or the intensity of IL-11Rα staining. This negative result is not unexpected, given that all patients with metastatic disease share a poor prognosis and short overall survival. A relatively small cohort of patient samples, such as that analyzed in the present study, is expected given the rare incidence of osteosarcoma (1). This caveat notwithstanding, our results suggest that IL-11Rα expression increases with tumor progression and is inversely correlated with overall survival.

An IL-11Rα:IL-11 Autocrine Loop Is Up-Regulated in Human Metastatic Osteosarcoma Cell Lines. Having demonstrated that IL-11Rα is an osteosarcoma biomarker related to disease progression and prognosis in patients, we next sought to investigate its functional role. We first evaluated IL-11Rα levels by flow cytometry in a panel of human osteosarcoma cell lines that are either nonmetastatic (HOS, MG63, CCH-OS-O, TE-85, and Saos-2) or metastatic (KRIB, SJSA1, CCH-OS-D, and LM7) to the lungs in animal models. We found a substantially higher proportion of osteosarcoma cells expressing IL-11Rα on the surface in all of the metastatic cell lines compared with the nonmetastatic cell lines (Fig. 2*A*). This finding was paralleled by an increase in mRNA levels, as quantified by quantitative PCR (qPCR) (Fig. 2*B*), suggesting that IL-11Rα is regulated at the transcriptional level in osteosarcoma cell lines.

We next quantified the levels of the IL-11Rα ligand IL-11 in conditioned media from the same cell lines by ELISA. Compared with nonmetastatic cells, increased levels of IL-11 were secreted by virtually all metastatic cell lines, with the exception of CCH-OS-D (Fig. 2*C*). This increase was also paralleled at the mRNA level (Fig. 2*D*). Some other negative control cytokines [i.e., granulocyte macrophage colony-stimulating factor (GM-CSF), IL-1β, IL-2, IL-6, IL-8, IL-10, IL-12, and tumor necrosis factor α (TNFα)] were not overexpressed in metastatic vs. nonmetastatic human osteosarcoma cell lines, as evaluated by multiplex ELISA (Meso Scale Discovery) (Fig. S1). Taken together, these data reveal the specific up-regulation of an IL-11Rα:IL-11 autocrine loop in human metastatic osteosarcoma cell lines, further supporting a functional role for IL-11Rα in the progression of human osteosarcoma.

IL-11Rα Signaling Is Necessary for Human Metastatic Osteosarcoma Cell Proliferation, Invasion, and Anchorage-Independent Growth. IL-11 induces a signaling cascade that leads to STAT3 activation by phosphorylation (12, 13). Therefore, we evaluated whether STAT3 could

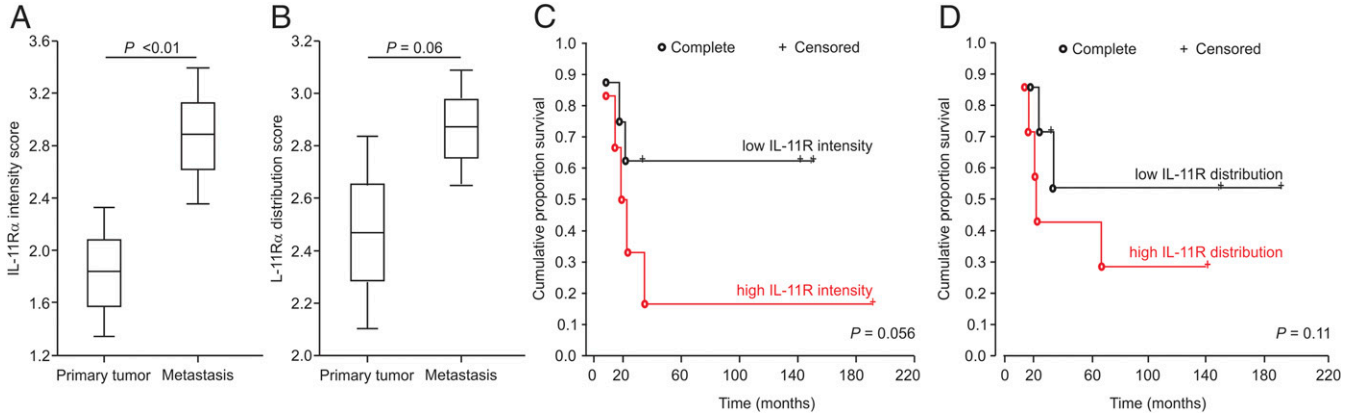

Fig. 1. Expression of IL-11Rα and IL-11 in human osteosarcoma specimens and correlation with disease progression. In analysis of a TMA composed of 18 primary osteosarcomas and 27 lung metastases immunostained for IL-11Rα, specific IHC signals were scored on both intensity (*A*) and distribution (*B*). Patient specimens were stratified based on their intensity (*C*) or distribution (*D*) score. Kaplan–Meier survival plots were drawn including both complete and censored data for all available patients ($n = 14$ primary osteosarcomas), and correlations were analyzed by Cox's F test and the log-rank test.

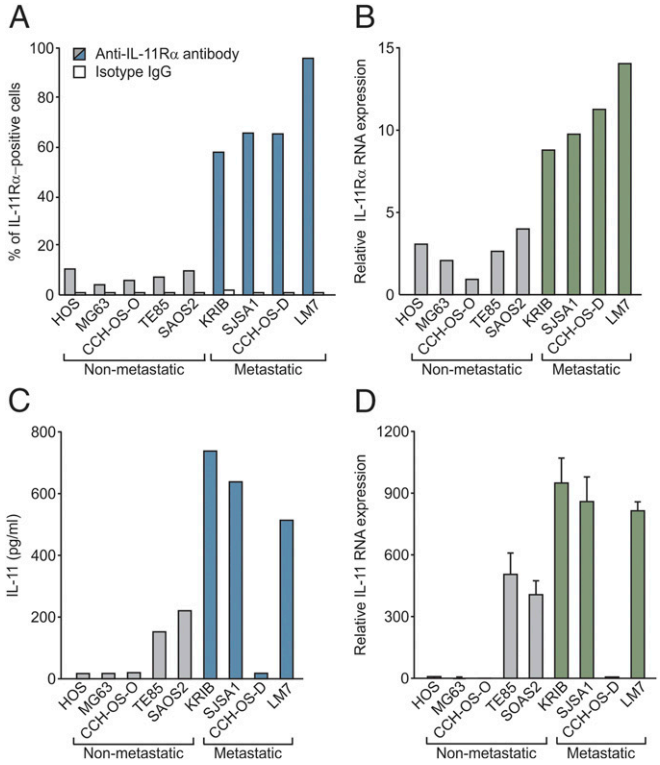

Fig. 2. Expression of IL-11Rα and IL-11 in a panel of human osteosarcoma cell lines. (*A*) Tumor cell-surface expression of IL-11Rα was assayed by flow cytometry and expressed as percent positive cells. (*B*) Total IL-11Rα mRNA was quantified by qPCR and normalized to the lowest value, arbitrarily set to 1. (*C*) Secreted IL-11 protein levels were quantified by ELISA in conditioned media and expressed in pg/mL. (*D*) Total IL-11 mRNA levels were quantified as in *B* and were repeated three times, with similar results.

be activated in exemplary nonmetastatic (HOS) and metastatic (CCH-OS-D) human osteosarcoma cells on IL-11 stimulation. CCH-OS-D cells were chosen because of the lower levels of IL-11 expressed and released in their conditioned culture medium (Fig. 2 *C* and *D*), which avoids receptor activation by the endogenous ligand. Cells were incubated with recombinant human IL-11 (rhIL-11; 25 ng/mL for 5 min), and fractionated protein extracts (total, cytoplasmic, and nuclear) were subjected to immunoblotting with an anti-phosphorylated STAT3 (pSTAT3 Tyr^{705}) antibody. In both cell lines, treatment with rhIL-11 induced approximately fourfold phosphorylation and specific nuclear accumulation of STAT3 compared with the nuclear marker poly(ADP-ribose) polymerase 1 (PARP-1) (Fig. 3*A*). These data suggest that IL-11Rα is functional in both nonmetastatic and metastatic settings.

To obtain a cellular model with controlled IL-11Rα amounts and functionality, we silenced IL-11Rα expression in KRIB cells, which is another suitable metastatic osteosarcoma cell line because it (*i*) expresses high levels of both IL-11Rα and IL-11 (Fig. 2), (*ii*) can be easily transduced in vitro, and (*iii*) enables both in vitro and in vivo experiments (16, 17). Silencing of IL-11Rα with two alternative shRNA constructs was confirmed by mRNA quantification (Fig. 3*B*) and protein immunoblotting (Fig. 3*C*). A corresponding decrease in pSTAT3 levels was observed, representative of the functional impairment of downstream signaling (Fig. 3*C*).

We next evaluated nontransduced, control shRNA-transduced, and IL-11Rα shRNA-transduced KRIB cells for metastasis-related phenotypes, including cell invasion and growth in soft agar. Silencing of IL-11Rα resulted in decreased cell proliferation (Fig. 3*D*) and invasion both at the basal level and in response to 50 mg/mL rhIL-11 (Fig. 3*E*). Consistently, IL-11Rα–silenced cells were less able to grow in an anchorage-independent fashion and to form colonies in soft agar in the presence of 50 mg/mL rhIL-11 (Fig. 3*F*). Collectively, these data indicate that IL-11Rα specifically regulates metastatic attributes in human osteosarcoma cells.

IL-11Rα Is Functionally Involved in Lung Colonization by Human Osteosarcoma Cells in Preclinical Models. We next investigated the functional role of IL-11Rα in vivo. To obtain an animal model of human metastatic osteosarcoma, nontransduced, control shRNA-transduced, and IL-11Rα shRNA-transduced KRIB cells were transfected with a luciferase reporter gene cassette before orthotopic intratibial administration in cohorts of nude mice. Six weeks later, lungs were explanted, and luciferase-expressing KRIB cells were visualized in an ex vivo IVIS imaging system (Xenogen) (Fig. 4*A*). Quantification of luminescent signals (*SI Results*) revealed decreased lung colonization by KRIB cells in which IL-11Rα had been silenced with either shRNA compared with either parental or control cells (Fig. 4*B*). This result was further confirmed by histological analysis of hematoxylin and eosin (H&E)-stained formalin-fixed, paraffin-embedded (FFPE) tissue sections (Fig. 4*C*), as well as quantification of micrometastatic foci in the lungs (Fig. 4*D*). These data demonstrate that IL-11Rα functions in the process of lung colonization during the secondary spread of human osteosarcoma cells in vivo. Moreover, our results support the validity of this orthotopic mouse model as a co-clinical trial surrogate of osteosarcoma progression in patients.

The IL-11Rα–Targeting Drug BMTP-11 Inhibits Primary Tumor Growth and Metastatic Spread of Human Osteosarcoma Cells in Preclinical Models. We have previously designed and validated the tumor-targeting small-molecule drug BMTP-11 (18), which consists of a functional IL-11Rα–binding peptide (CGRRAGGSC) (15) fused to the apoptosis-inducing peptidomimetic $_D(KLAKLAK)_2$ (19). The antitumor activity of BMTP-11 has been previously evaluated in preclinical models of solid tumors with propensity to metastasize to bone, such as prostate cancer (20) and lung cancer (21), and also in hematologic malignancies primarily originated within the bone marrow cavity, such as leukemia (18); moreover, we have recently reported a first-in-man clinical trial in patients with metastatic prostate cancer (20).

Given our promising and consistent observations from tumor cell lines, animal models, and human osteosarcoma specimens (11), along with the data presented here, we also evaluated the preclinical efficacy of BMTP-11 in a orthotopic model of human metastatic osteosarcoma. At 2 wk postimplantation, nude mice with established KRIB tumors were randomized ($n = 5$ mice per group) to receive control (vehicle), the chemotherapeutic drug gemcitabine i.p., BMTP-11 delivered either i.v. or intranasally, or BMTP-11 i.v. plus gemcitabine i.p. twice weekly for 30 d. Tumor size was measured with calipers at days 7, 14, 20, 24, and 30. Tumor growth (weight and volume) was inhibited on BMTP-11 or gemcitabine treatment compared with the control group (Fig. 5 *A*–*C*). The combination treatment BMTP-11 plus gemcitabine provided increased efficacy compared with each single agent alone. FFPE tumor sections were stained for either terminal deoxynucleotidyl transferase dUTP nick-end labeling (TUNEL) or cleaved caspase-3 as apoptosis markers. We found increased apoptotic indexes specifically in response to BMTP-11–based treatments (Fig. 5*D*). Metastatic spread to the lungs was also evaluated on explanted tissues at the end of the experiment. BMTP-11–based treatments resulted in significant decreases in the gross macroscopic area (Fig. 5*E*) and number (Fig. 5*F*) of microscopic pulmonary foci. Collectively, these data demonstrate the efficacy of BMTP-11 in inducing apoptosis in osteosarcoma cells, thus delaying primary tumor growth and secondary metastatic spread to the lungs.

We chose gemcitabine as a reference cytotoxic because it was previously evaluated in patients with doxorubicin-resistant osteosarcoma (22). Moreover, recent retrospective studies in small cohorts of pediatric osteosarcoma patients indicate activity of gemcitabine-based regimens as second- or later-line chemotherapy for very-high-risk (relapsed, metastatic, inoperable)

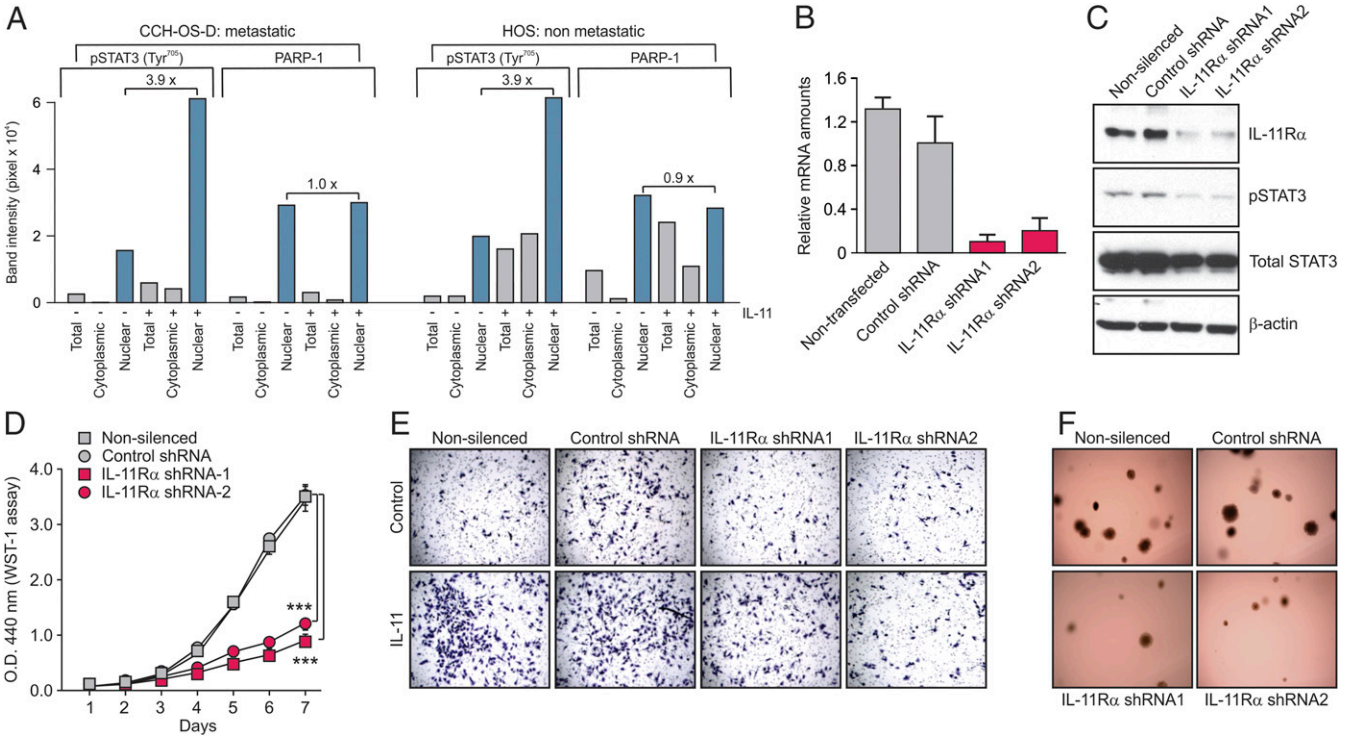

Fig. 3. Impairment of in vitro functions of human osteosarcoma cells on silencing of IL-11Rα. (*A*) Evaluation of the IL-11Rα:IL-11 signaling pathway in nonsilenced osteosarcoma cells was done by quantifying STAT3 phosphorylation and nuclear accumulation in CCH-OS-D (metastatic) and HOS (nonmetastatic) cell lines in response to rhIL-11 (25 ng/mL for 5 min). Fractionated protein extracts were subjected to immunoblotting with an anti-pSTAT3 (Tyr^{705}) antibody, and band intensity was quantified by densitometry with ImageJ software. Staining for the nuclear marker PARP-1 served as an internal reference. (*B* and *C*) KRIB cells were stably silenced by infection with two alternative shRNA lentiviral vectors, IL-11Rα shRNA1 and shRNA2, followed by quantification of IL-11Rα mRNA by qPCR (*B*) and of protein by immunoblotting (*C*). Nonsilenced cells and cells silenced with control shRNA served as references. pSTAT3 levels were assayed to confirm the impairment of IL-11Rα signaling in silenced cells. (*D–F*) All KRIB cell variants were challenged in proliferation (WST-1) (*D*), invasion (Matrigel-coated transwells) in the basal condition or in the presence of rhIL-11 (50 ng/mL) (*E*), and colony-forming (soft agar) in vitro assays in the presence of rhIL-11 (50 ng/mL) (*F*). In *E* and *F*, representative images are shown. (Original magnification: 5× in *E*; 10× in *F*.) In *D*, $***P < 0.001$ by one-way ANOVA followed by Bonferroni's posttest. The experiments were repeated three times, with similar results.

tumors (6, 7). Given the synergy documented in the present work, the use of gemcitabine as backbone for a chemotherapeutic doublet with BMTP-11, or the potential development of a three-drug regimen with the incorporation of a taxane such as docetaxel (6, 23, 24), might be evaluated in the setting of MAP failures or tumor recurrences.

Taken together, our findings in this work establish that targeting the IL-11:IL-11Rα axis is a potential clinical strategy for therapeutic intervention in osteosarcoma. Our findings further support the value of BMTP-11 as prospective drug for treating osteosarcoma, in addition to the preclinical and translational data for other more common solid and hematologic tumors (18, 20, 21).

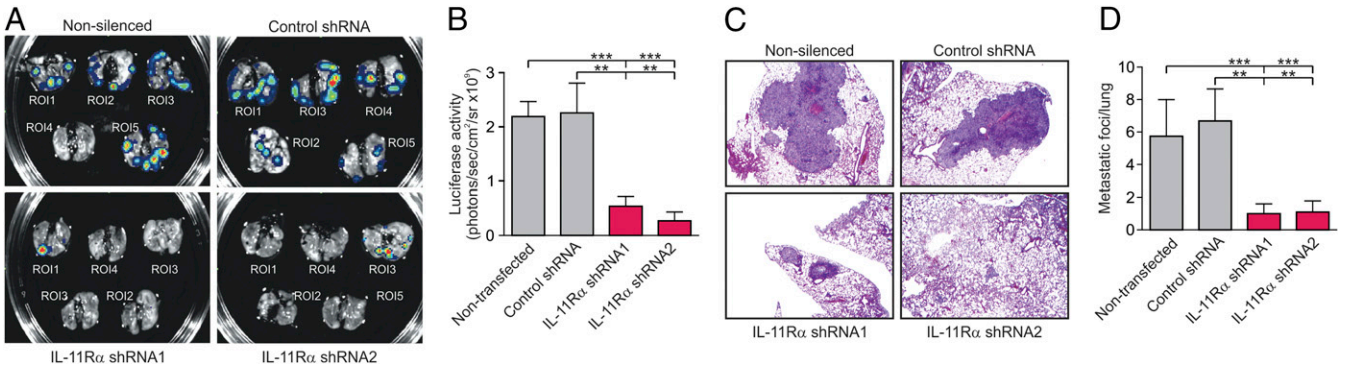

Fig. 4. Impairment of in vivo functions of human metastatic osteosarcoma cells on silencing of IL-11Rα. Nontransduced, control shRNA-transduced, and IL-11Rα shRNA-transduced KRIB cells were transfected with a luciferase gene cassette, followed by intratibial administration in nude mice. (*A*) Ex vivo IVIS imaging of lungs explanted after 6 wk. ROI, region of interest. (*B*) Quantification of luciferase activity values (photons/s/cm²/sr). (*C*) H&E staining of explanted lungs. (*D*) Quantification of metastatic foci by histopathological analysis. In *C*, representative pictures are shown. (Original magnification: 10×.) In *B* and *D*, $**P < 0.01$, $***P < 0.001$ by one-way ANOVA followed by Bonferroni's posttest. The experiments were repeated three times, with similar results.

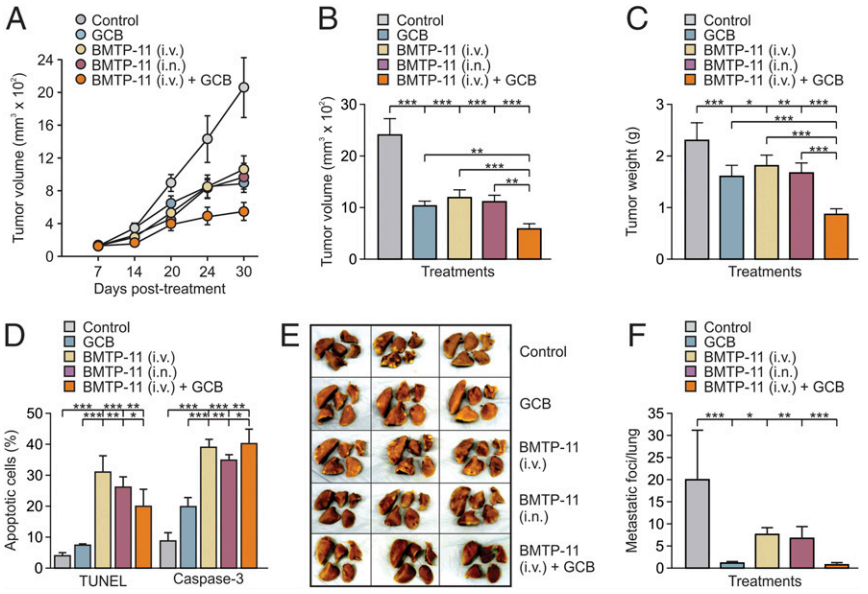

Fig. 5. BMTP-11 inhibits primary tumor growth and metastatic spread to the lungs by inducing apoptosis in human osteosarcoma cells. (*A*–*C*) Delay in primary tumor growth by BMTP-11–based treatments. Nude mice with established intratibial KRIB tumors (n = 5 mice/group; mean tumor size, ~4–5 mm^3) were treated with: control (vehicle only), 120 μg/kg body weight gemcitabine (GCB), 300 μg/animal BMTP-11 i.v., 300 μg/animal BMTP-11 intranasally, or 300 μg/animal BMTP-11 i.v. plus 120 μg/kg body weight GCB, twice weekly for a total of 30 d. (*A*) Tumor volumes measured with calipers at the indicated time points. (*B* and *C*) Tumor volumes (*B*) and tumor weights (*C*) at endpoint. (*D*) Apoptotic indexes derived by quantification of TUNEL or cleaved caspase-3 immunostaining on FFPE tumor sections (n = 3). (*E* and *F*) Delay in metastatic spread to the lungs by BMTP-11–based treatments. (*E*) Lungs explanted at day 30 posttreatment. Representative pictures from three mice per group are shown. (*F*) Quantification of metastatic foci by histopathological analysis of H&E-stained FFPE sections of explanted lungs. In *B*, *C*, *D*, and *F*, $*P < 0.05$, $**P < 0.01$, $***P < 0.001$ by one-way ANOVA followed by Bonferroni's posttest. The experiment was repeated three times, with similar results.

Methods

Cell Culture. HOS, MG-63, TE85, Saos-2, KRIB, and SJSA-1 cell lines were obtained from American Type Culture Collection. CCH-OS-O and CCH-OS-D were derived from patient specimens at the Children's Cancer Hospital, University of Texas M.D. Anderson Cancer Center (13), and the metastatic LM7 cell line was developed by successive reimplants of Saos-2 cells through the lungs of nude mice (17). Cells were maintained at 37 °C in 5% CO_2 in DMEM with 10% FBS and 10 mg/mL penicillin-streptomycin.

TMA Preparation and IHC. FFPE specimens of primary tumors (n = 18) and lung metastases (n = 27) from the osteosarcoma database and hospital tumor registry were used to build a TMA following the guidelines recommended by the Tissue Array Research Program of the National Cancer Institute. This study adhered strictly to current medical ethics recommendations and guidelines on human research, and the protocol was reviewed and approved by the Clinical Ethics Service, Institutional Biohazard Committee, Clinical Research Committee, and Institutional Review Board at each of the respective participating institutions. All patients signed an informed consent prior to the beginning of the study. Four-micrometer sections were subjected to antigen retrieval by heat with EDTA (pH 8.0; Zymed), followed by biotin and protein blocking (Dako). EDTA was chosen for its documented preservation of antigens even in the process of tissue decalcification (25). Expression of IL-11Rα was evaluated with a rabbit anti–IL-11Rα antibody (C20; Santa Cruz Biotechnology) diluted at 1:15 (vol/vol) and incubated for 45 min, followed by development with the LSAB+ Kit (Dako). Staining was evaluated by two independent pathologists and graded for both intensity and distribution of staining as described previously (11).

Flow Cytometry. Cells were suspended in a fluorescence-activated cell sorting (FACS) buffer consisting of PBS with 2% FBS, followed by incubation with 1 mg/mL of either phycoerythrin (PE)-conjugated anti–IL-11Rα antibody or isotype-matched, PE-conjugated IgGs (Pharmingen) for 30 min at 4 °C. After washing in FACS buffer, cells were acquired with a FACSCalibur cell analyzer (BD Biosciences), and analyzed with using CellQuest version 3.3 (BD Biosciences).

RNA Isolation and qPCR. Here, 1 μg of total RNA isolated with a Qiagen kit was amplified with IL-11RA (Assay ID: Hs00234415_m1; Thermo Fisher Scientific) with the AgPath-ID One-Step RT-PCR reagents (Applied Biosystems) in an ABI PRISM 7500 PCR system (Applied Biosystems). Gene expression was calculated by the comparative delta-delta cycle threshold (ΔΔCt) method, and cyclophilin A served as an endogenous control reference.

Cytokine Quantification by ELISA. Conditioned media were collected from cells grown in T-25 flasks and maintained for 24 h in serum-free medium, centrifuged at 1,000 × g for 10 min, pooled, aliquoted, and frozen at –80 °C until use. Total levels of secreted IL-11 protein were measured with the Quantikine ELISA Human IL-11 Kit (R&D Systems). A cytokine panel including GM-CSF, IL-1β, IL-2, IL-6, IL-8, IL-10, IL-12, and TNFα was analyzed by multiplex ELISA (Meso Scale Discovery).

Generation of IL-11Rα–Silenced Cells and Luciferase-Expressing Cells. First, 293T cells were transfected with IL-11Rα–specific (GE Healthcare) and control GIPZ lentiviral shRNA plasmids (Dharmacon), together with packaging vectors, following the manufacturer's instructions. At 48–72 h posttransfection, viral particle-containing supernatants were collected, filtered through 0.45-μm-pore filters, and used to infect KRIB cells in the presence of 8 μg/mL polybrene (Sigma-Aldrich). After another 72 h, shRNA-transduced GFP-expressing cells were separated by cell sorting with a BD FACSAria instrument (BD Biosciences), and IL-11Rα silencing was confirmed by qPCR and immunoblotting. To obtain luciferase-expressing cells for ex vivo imaging studies, KRIB cells were transfected with a recombinant retroviral plasmid carrying a luciferase gene cassette into a pLazarus vector (26).

Immunoblot Analysis. Osteosarcoma cells were treated with 25 ng/mL rhIL-11 (R&D Systems) for 5 min, followed by lysis in radioimmunoprecipitation assay (RIPA) buffer (50 mM Tris·HCl pH 7.4, 1% Nonidet P-40, 0.5% Na-deoxycholate, 0.1% SDS, 150 mM NaCl, 2 mM EDTA, and 50 mM NaF) supplemented with protease and phosphatase inhibitors (Sigma-Aldrich). Protein concentration was determined by the bicinchoninic acid protein assay (Thermo Fisher Scientific). Denatured samples were separated on 10% SDS/PAGE gels and blotted to nitrocellulose membranes. Membranes were blocked in 5% (g/vol) nonfat milk in Tris-buffered saline containing 0.1% (vol/vol) Tween-20 (TBST). Primary antibodies against IL-11Rα (Abcam); pSTAT3, STAT3, PARP-1, and α-tubulin (Cell Signaling Technology); and β actin (Sigma-Aldrich) were diluted in TBST containing 2.5% (g/vol) nonfat milk and incubated at 4 °C overnight. After washing, membranes were incubated with horseradish peroxidase-conjugated secondary antibodies (1:200 vol/vol; GE Healthcare Life Sciences) for 1 h at room temperature. Chemiluminescent detection was performed with the SuperSignal West Dura Extended Duration Kit (Thermo Fisher Scientific). Band intensity was quantified by densitometry with ImageJ software (27).

In Vitro Cell Assays. For proliferation assays, KRIB cells were grown in 24-well plates in DMEM supplemented with 10% FBS, and viability was evaluated with WST-1 reagent (Sigma-Aldrich) following the manufacturer's instructions. For invasion assays, 8-μm Transwells were coated with Matrigel, and KRIB cells were seeded onto the upper chamber in DMEM supplemented with 10% FBS only (control) or with 50 ng/mL rhIL-11 in 10% FBS. After 48 h, noninvaded cells were removed, and cells on the bottom side of the wells were fixed in PBS containing 3% (g/vol) paraformaldehyde, stained with crystal violet, photographed, and counted under a light microscope (Olympus). To evaluate anchorage-independent growth, KRIB cells (5×10^4) were suspended in DMEM supplemented with 10% FBS and containing 0.3% (g/vol) agarose, and then seeded into 12-well plates onto a solidified layer of 0.6% (g/vol) low-melting-point agarose in DMEM. Cultures were maintained in DMEM supplemented with 10% FBS and containing 50 ng/mL rhIL-11. After 3 wk, colonies ≥0.2 mm in diameter were counted and photographed with an IMT-2 Olympus phase-contrast microscope.

Detection of Apoptotic Cells in Experimental Tumor Tissues. Cleaved caspase-3 was detected by IHC on FFPE sections of explanted tumors. Antigen retrieval was achieved in Borg Decloaker (BioCare Medical) at sub-boiling temperature, followed by protein block with 4% (g/vol) fish gelatin in PBS. Staining was performed by incubation with a rabbit polyclonal anti-cleaved caspase-3 antibody (1:100 vol/vol; BioCare Medical), followed by a biotinylated goat anti-rabbit secondary antibody (1:1,000 vol/vol; Vector Laboratories). Signals were revealed with the LSAB+ Kit (Dako) following Delco's instructions. Cells were randomly scored and analyzed by Sigma Plot software (28). A TUNEL assay was performed with the In Situ Cell Death Detection Kit (Roche) following Roche's instructions. Tissue sections were treated with proteinase K (10 μg/mL) for 20 min, washed twice with PBS, labeled, and stained with the TUNEL reaction mixture (label plus enzyme solution) for 60 min at 37 °C. A negative control without enzyme and a positive control with DNase I (3,000 U/mL) were also included. Slides were mounted in Vectashield medium with DAPI (Vector Laboratories). Apoptotic cells were counted with a fluorescent microscope (Leica).

Preclinical Orthotopic Models. The animal experiments were in full compliance with the Institutional Animal Care and Utilization Committee (IACUC) policies and procedures, following standard guidelines for the care and use of laboratory animals (29). Before initiation of experiments, all protocols and procedures with animals were properly reviewed and approved by IACUC. The 5-wk-old male nu/nu (nude) mice were purchased from the National Cancer Institute's Frederick Cancer Research Facility and maintained in a pathogen-free barrier animal facility approved by the American Association for Accreditation of Laboratory Animal Care. Animals were kept on a 12-h-light/dark cycle, with standard rodent chow and water available ad libitum.

Intratibial implantation of osteosarcoma cells (11) was with KRIB cells at 80% confluence after detaching with 0.25% (vol/vol) trypsin and 0.02% (g/vol) EDTA, washing in serum-free medium, and resuspending in HBSS before injection (5×10^4 cells/mouse) into the right tibia of nude mice. During all preimaging and surgical procedures, mice were anesthetized (2.5% vol/vol isoflurane in O_2 and nembutal 50 mg/kg i.p., respectively), with temperature maintained at 38 °C with a heat lamp.

Ex Vivo Bioluminescence Imaging. Mice were implanted with luciferase-expressing KRIB variants (nontransduced, control shRNA- transduced, IL-11Rα shRNA1– transduced, and shRNA2-transduced). At the endpoint, animals were injected s.c. with 15 mg/mL luciferin potassium salt in PBS at 150 mg/kg body weight. Ten minutes after luciferin injection, animals were killed and lungs explanted. Ex vivo bioluminescence imaging was performed in an IVIS 100 imaging system (Xenogen). A digital gray-scale image of the explanted lungs and a pseudocolor image of photons produced by active luciferase were analyzed with Living Image (Xenogen).

Preclinical Therapeutic Protocols. Mice were randomized when tumors reached a volume of 4–5 mm^3. BMTP-11 was administered either i.v. (300 μg/mouse in 100 μL of saline) or intranasally (300 μg/mouse in 15 μL of saline), and gemcitabine was administered i.p. (120 μg/kg body weight in 200 μL of saline). Control mice received saline on the same schedule (twice weekly for a total of 30 d). Primary tumor growth was measured with a caliper at the indicated days postimplantation. Mice were killed at day 30, and both primary tumors and lungs were explanted and processed (FFPE) for histopathological analysis.

Statistics. Differences in IL-11Rα expression between sample groups from patients in the TMA were evaluated by Student's *t* test. Patient-derived specimens were stratified based on their intensity or distribution score, and Kaplan-Meier survival plots were drawn of both complete and censored data. Given the relatively small numbers of patients tested, the study was underpowered, and differences between groups were evaluated by Cox's *F* and log-rank tests. For in vitro and in vivo experiments, data were analyzed by one-way ANOVA followed by Bonferroni's posttest and are presented as mean ± SD of three independent experiments. A P value < 0.05 was considered statistically significant. All statistical analyses were performed with Prism version 5.01 (GraphPad Software).

ACKNOWLEDGMENTS. We thank Dr. Helen Pickersgill (Life Science Editors) for editorial services and Ms. Guiying Wang for technical assistance. This work was supported by the Triumph Over Kid Cancer Foundation (V.O.L.), NIH Grants P30CA016672 and P30CA118100, the Gillson-Longenbaugh Foundation (R.P. and W.A.), a National Cancer Institute Cancer Center Support Grant (to University of New Mexico Comprehensive Cancer Center), and the Marcus Foundation (to University of Texas M.D. Anderson Cancer Center).

1. Ottaviani G, Jaffe N (2009) The epidemiology of osteosarcoma. *Cancer Treat Res* 152:3–13.
2. Bielack SS, et al. (2002) Prognostic factors in high-grade osteosarcoma of the extremities or trunk: An analysis of 1,702 patients treated on neoadjuvant cooperative osteosarcoma study group protocols. *J Clin Oncol* 20:776–790.
3. Meyers PA, et al. (2005) Osteosarcoma: A randomized, prospective trial of the addition of ifosfamide and/or muramyl tripeptide to cisplatin, doxorubicin, and high-dose methotrexate. *J Clin Oncol* 23:2004–2011.
4. Meyers PA, et al.; Children's Oncology Group (2008) Osteosarcoma: The addition of muramyl tripeptide to chemotherapy improves overall survival—a report from the Children's Oncology Group. *J Clin Oncol* 26:633–638.
5. Bielack SS, et al.; EURAMOS-1 Investigators (2015) Methotrexate, doxorubicin, and cisplatin (MAP) plus maintenance pegylated interferon alpha-2b versus MAP alone in patients with resectable high-grade osteosarcoma and good histologic response to preoperative MAP: First results of the EURAMOS-1 good response randomized controlled trial. *J Clin Oncol* 33:2279–2287.
6. Palmerini E, et al. (2016) Gemcitabine and docetaxel in relapsed and unresectable high-grade osteosarcoma and spindle cell sarcoma of bone. *BMC Cancer* 16:280.
7. Kuo C, et al. (2017) Docetaxel, bevacizumab, and gemcitabine for very high risk sarcomas in adolescents and young adults: A single-center experience. *Pediatr Blood Cancer* 64. doi: 10.1002/pbc.26265.
8. Grignani G, et al.; Italian Sarcoma Group (2015) Sorafenib and everolimus for patients with unresectable high-grade osteosarcoma progressing after standard treatment: A non-randomised phase 2 clinical trial. *Lancet Oncol* 16:98–107.
9. Safwat A, Boysen A, Lücke A, Rossen P (2014) Pazopanib in metastatic osteosarcoma: Significant clinical response in three consecutive patients. *Acta Oncol* 53:1451–1454.
10. Wagner LM, et al. (2015) Phase II study of cixutumumab in combination with temsirolimus in pediatric patients and young adults with recurrent or refractory sarcoma: A report from the Children's Oncology Group. *Pediatr Blood Cancer* 62:440–444.
11. Lewis VO, et al. (2009) The interleukin-11 receptor alpha as a candidate ligand-directed target in osteosarcoma: Consistent data from cell lines, orthotopic models, and human tumor samples. *Cancer Res* 69:1995–1999.
12. Campbell CL, Jiang Z, Savarese DM, Savarese TM (2001) Increased expression of the interleukin-11 receptor and evidence of STAT3 activation in prostate carcinoma. *Am J Pathol* 158:25–32.
13. Huang G, et al. (2012) Genetically modified T cells targeting interleukin-11 receptor α-chain kill human osteosarcoma cells and induce the regression of established osteosarcoma lung metastases. *Cancer Res* 72:271–281.
14. Liu T, et al. (2015) Interleukin-11 receptor α is overexpressed in human osteosarcoma, and near-infrared-labeled IL-11Rα imaging agent could detect osteosarcoma in mouse tumor xenografts. *Tumour Biol* 36:2369–2375.
15. Zurita AJ, et al. (2004) Combinatorial screenings in patients: The interleukin-11 receptor alpha as a candidate target in the progression of human prostate cancer. *Cancer Res* 64:435–439.
16. Berlin O, et al. (1993) Development of a novel spontaneous metastasis model of human osteosarcoma transplanted orthotopically into bone of athymic mice. *Cancer Res* 53:4890–4895.
17. Jia SF, Worth LL, Kleinerman ES (1999) A nude mouse model of human osteosarcoma lung metastases for evaluating new therapeutic strategies. *Clin Exp Metastasis* 17:501–506.
18. Karjalainen K, et al. (2015) Targeting IL11 receptor in leukemia and lymphoma: a functional ligand-directed study and hematopathology analysis of patient-derived specimens. *Clin Cancer Res* 21:3041–3051.
19. Ellerby HM, et al. (1999) Anti-cancer activity of targeted pro-apoptotic peptides. *Nat Med* 5:1032–1038.
20. Pasqualini R, et al. (2015) Targeting the interleukin-11 receptor α in metastatic prostate cancer: A first-in-man study. *Cancer* 121:2411–2421.
21. Cardó-Vila M, et al. (2016) Interleukin-11 receptor is a candidate target for ligand-directed therapy in lung cancer: Analysis of clinical samples and BMTP-11 preclinical activity. *Am J Pathol* 186:2162–2170.
22. Merimsky O, et al. (2000) Gemcitabine in bone sarcoma resistant to doxorubicin-based chemotherapy. *Sarcoma* 4:7–10.
23. Lee JA, et al. (2016) Higher gemcitabine dose was associated with better outcome of osteosarcoma patients receiving gemcitabine-docetaxel chemotherapy. *Pediatr Blood Cancer* 63:1552–1556.
24. Navid F, et al. (2008) Combination of gemcitabine and docetaxel in the treatment of children and young adults with refractory bone sarcoma. *Cancer* 113:419–425.
25. Bussolati G, Leonardo E (2008) Technical pitfalls potentially affecting diagnoses in immunohistochemistry. *J Clin Pathol* 61:1184–1192.
26. Nyati MK, et al. (2002) The potential of 5-fluorocytosine/cytosine deaminase enzyme prodrug gene therapy in an intrahepatic colon cancer model. *Gene Ther* 9:844–849.
27. Schindelin J, et al. (2012) Fiji: An open-source platform for biological-image analysis. *Nat Methods* 9:676–682.
28. Gown AM, Willingham MC (2002) Improved detection of apoptotic cells in archival paraffin sections: Immunohistochemistry using antibodies to cleaved caspase 3. *J Histochem Cytochem* 50:449–454.
29. Committee for the Update of the Guide for the Care and Use of Laboratory Animals, Institute for Laboratory Animal Research, Division on Earth and Life Studies, National Research Council of the National Academies of Sciences (2011) *Guide for the Care and Use of Laboratory Animals* (National Academies Press, Washington, DC), 8th Ed.